Enhancing efficiency and economics of phosphorus recovery process by customizing the product based on sidestream characteristics – an alternative phosphorus recovery strategy

Sina Shaddel, Seniz Ucar, Jens-Petter Andreassen and Stein W. Østerhus

ABSTRACT

The enhanced biological phosphorus removal process makes the phosphorus recovery feasible from the dewatering streams of biological sludge. The physicochemical properties of these sidestreams, as an input to a crystallizer, are different before and after anaerobic digestion. In this study, phosphorus recovery by calcium phosphate is proposed for pre-digestion sidestreams and by struvite precipitation for post-digestion sidestreams. The thermodynamic modeling followed by experimental tests was performed to evaluate the recovery efficiency and product properties of struvite and calcium phosphates. The variations in phosphorus recovery potential, reaction kinetics and particle size distribution emphasize the importance of the adjustment of initial supersaturation and pH of the reaction. The optimum pH, considering the economics and recovery efficiency, for both calcium phosphate and struvite precipitation was found to be pH = 8.5, whereas further increase of pH will not improve the overall efficiency of the process. In the case of calcium phosphate precipitation, it was shown that possible phase transformations should be considered and controlled as they affect both process efficiency and product properties. The economic evaluation indicated that the optimized operational condition should be determined for the phosphorus recovery process and that chemical costs for the production of calcium phosphates is lower than for struvite.

Key words | calcium phosphate, crystallization, economics, phosphorus recovery, process efficiency, struvite

Sina Shaddel (corresponding author)
Stein W. Østerhus
Department of Civil and Environmental Engineering,
Norwegian University of Science and Technology (NTNU),
Trondheim,
Norway
E-mail: *sina.shaddel@ntnu.no*

Seniz Ucar
Jens-Petter Andreassen
Department of Chemical Engineering,
Norwegian University of Science and Technology (NTNU),
Trondheim,
Norway

INTRODUCTION

Phosphate rocks are the main source of phosphorus for most phosphorus fertilizers in modern agriculture. The quantitative and qualitative reduction of the primary phosphorus rock reserves has led to great interest in phosphorus recovery from secondary resources to ensure sustainable food production in the future. The sewage sludge is a rich secondary resource for phosphorus and the enhanced biological phosphorus removal (EBPR) process provides great potential for phosphorus recovery from sludge phase (Wan *et al.* 2013). The sidestreams of the sludge handling line in the EBPR process, both before and after anaerobic digestion, are rich in phosphate. The high phosphate concentration and small volume of these sidestreams make them attractive for phosphorus recovery by chemical precipitation.

The precipitation of struvite and different calcium phosphate compounds is widely studied for phosphorus recovery from wastewater (Mehta *et al.* 2015; Melia *et al.* 2017). In these studies, input material is the liquid phase of anaerobically digested sludge and P-recovery from phosphate-rich sidestreams of undigested sludge is not fully elucidated. Anaerobic digestion of sludge and the conceivable introduction of ammonium recovery in the process change the physical and chemical properties of these sidestreams. Therefore, adaption of final product to the physicochemical properties of the targeted sidestream is necessary for an effective phosphorus recovery process.

doi: 10.2166/wst.2019.178

The aim of this study is to evaluate P-recovery in pre-digestion and post-digestion mode. For this purpose, calcium phosphates are selected as the targeted product for sidestreams with low ammonium content, and struvite for sidestreams after anaerobic digestion with higher ammonium content. The assessment is based on the phosphorus recovery efficiency, economic feasibility and product properties such as purity, water content and particle size.

The anaerobic character of thickening and dewatering of EBPR sludge leads up to PO_4^{3-}-release to the sludge dewatering sidestream. Application of a P-stripper with proper retention time and adequate amount of volatile fatty acid will improve the PO_4^{3-}-release to the liquid phase at dewatering stage of undigested EBPR sludge. An acid digester has also been proposed to facilitate the PO_4^{3-}-release and dissolution of the crystallized and organically bound phosphorus in this stage (Li *et al.* 2018). However, the low ammonium content of these sidestreams makes them less suitable for struvite precipitation while P-recovery by calcium phosphates can offer a noteworthy advantage. The precipitation of phosphorus in this stage diverts the soluble-P from the digester and lowers the risk of unwanted precipitation during digestion and post-digestion operations. The P-recovery by calcium phosphate at low pH (i.e. pH = 5–7, low NH_4-content) on P-rich sidestreams of undigested sludge will reduce the soluble-P in the digester, improve the dewaterability of the sludge and reduce the total-P in the biosolids (Li *et al.* 2018). The pre-digestion P-recovery by calcium phosphates at low pH can reduce the CO_2 footprint of the process. This is due to less consumption of sodium hydroxide (NaOH) and less polymer consumption for sludge dewatering. The CO_2 footprint in the production of NaOH is several times higher than that in the production of $CaCl_2$ or $MgCl_2$ (Thannimalay *et al.* 2013).

Degradation of sludge substrate to methane and CO_2 in anaerobic digestion increases the carbonate content in the sludge dewatering sidestream (Chipasa 2003). The coexisting carbonates (CO_3^{2-}), resulting from CO_2 dissolution, and production of amino groups (-NH_2) and ammonium increase the alkalinity of the dewatering sidestream from anaerobically digested sludge with respect to the undigested one (Möller & Müller 2012). The higher ammonium concentration increases the nucleation pH of calcium phosphates, and was shown to reduce the growth rate of brushite ($CaHPO_4{\cdot}2H_2O$) and hydroxyapatite ($Ca_{10}(PO_4)_6(OH)_2$) (Vasenko & Qu 2017). Moreover, the required amount of caustic chemicals for pH elevation increases since the ammonium reaction tends to neutralize the hydroxyl ions (Gerardi 2003). However, increased ammonium concentration in solution boosts both the nucleation and growth kinetics of struvite precipitation. Therefore, the sidestreams after anaerobic digestion are better alternatives for struvite precipitation. In addition to anaerobic digestion, thermochemical treatments (incineration, liquefaction, gasification, pyrolysis) and hydrothermal treatments (thermal hydrolysis, wet oxidation) are among emerging techniques to treat sludge with phosphate release to aqueous phase (Munir *et al.* 2017).

Phosphorus recovery from the sidestreams of undigested sludge can be advantageous also from other aspects. The reduction of phosphate load to the anaerobic digester is proposed as an effective sludge handling strategy since during the anaerobic digestion a fraction of dissolved-P will mineralize and associate with suspended solids (Wilfert *et al.* 2018). This P-loss, which can be lower than 10% and up to 36%, will decrease the water-extractable P-fraction for further crystallization (Warren 1981; Massé *et al.* 2007; Marcato *et al.* 2008). The addition of iron or aluminum salts as support for an EBPR process to meet the effluent requirements or to resolve the sulfide production and odor problems is a common practice (Frossard *et al.* 1997; Wilfert *et al.* 2018). However, these ions will strongly reduce the availability of soluble phosphorus for further recovery. In these cases, P-recovery by calcium phosphate precipitation at the P-rich sidestreams of thickened bio-P sludge is still feasible.

In the context of a circular economy to achieve a sustainable phosphorus chain, the recovered phosphorus requires conversion into products that have diverse applications. Struvite, due to being composed of primary macronutrients (N and P) and secondary macronutrient (Mg), is a potential fertilizer while calcium phosphates have the potential to be used as secondary materials for the phosphorus industry since they are directly comparable to phosphate rocks. Calcium phosphates that precipitated from the wastewater can be mixed with normally mined phosphate rocks in fertilizer factories if they meet the standards for rocks (i.e. magnesium content, organic contamination). However, struvite, unlike calcium phosphates, is not suitable as an alternative raw material in electro-thermal processes because of its ammonia content (Cornel & Schaum 2009). Further, phosphorus recovery by calcium phosphates may make economic sense for small-scale wastewater treatment plants (Law & Pagilla 2018). Calcium phosphate compounds are potential alternatives for P-recovery when nitrogen is not available in the targeted stream such as industrial wastewater treatment plants, which in many cases do not accept nitrogen compounds since they do not have a biological treatment (Cichy *et al.* 2019).

The recovery of phosphorus in the form of high purity chemicals for applications in agriculture and industry will

improve the economics of the phosphorus recovery process (Vasenko & Qu 2017). The affinity of heavy metals is higher for volatile organic solids than for inert solids (Gould 1977). Due to degradation of volatile organic solids in the anaerobic digester, a higher concentration of heavy metals is expected in the dewatering sidestream of anaerobically digested sludge. Thus, in the case that contamination of final product by heavy metals is a concern, pre-digestion P-recovery can reduce this risk. Different forms of calcium phosphates have different potential for inorganic and organic contamination. Therefore, it is important to consider the phase transformation of calcium phosphates during precipitation from wastewater (Monballiu *et al.* 2018). However, this aspect is little studied for the wastewater applications.

The aim of this study is to evaluate the P-recovery efficiency, product properties and economics of the P-recovery process by struvite and calcium phosphate precipitation. The assessment of calcium phosphates and struvite under similar conditions enables us to select the proper product based on the physicochemical properties of the input material to the crystallizer. Further, this study aims to propose a alternative P-recovery strategy to improve the process flexibility and to improve the overall efficiency and economics of the P-recovery process. The proposed alternative strategy is to select the final product based on the characteristics of the sludge dewatering sidestream before and after anaerobic digestion. For this purpose, we performed a series of lab-scale crystallization experiments of struvite and calcium phosphates. The potential phosphorus recovery is calculated by thermodynamic equilibrium calculations followed by experimental validation of the results. The product properties such as phase characterization, morphology, particle size and dewaterability of obtained products are presented. The economic evaluation is also presented based on the obtained results in this study. The results of this study can be used for optimization of efficiency and economics of the phosphorus recovery processes.

MATERIALS AND METHODS

Materials

Magnesium chloride hexahydrate ($MgCl_2{\cdot}6H_2O$), ($CaCl_2$), sodium dihydrogen phosphate dihydrate ($NaH_2PO_4{\cdot}2H_2O$), ammonium chloride (NH_4Cl) and NaOH were used for the synthesis of struvite and calcium phosphates. All chemical reagents were purchased from Merck and were analytical grade, unless stated otherwise. Milli-Q water (18.2 MΩ·cm) was used for all purposes.

Methods

All experiments were carried out using a lab-scale crystallization system, composed of a 1 L glass reactor, stirred with a Teflon two-blade propeller controlled by a mechanical stirrer operated at 200 rpm. Temperature was regulated by a water bath and maintained at 20 ± 0.5 °C for all experiments. The pH was constantly measured and recorded by a combined glass electrode with KCl reference electrolyte connected to EasyDirect™ pH software (Metrohm), and calibrations were carried out daily. In the case of constant pH experiments, the pH was maintained by addition of 1 M NaOH. Nitrogen atmosphere presaturated with water was constantly preserved on top of the solutions throughout the crystallization reactions to prevent intrusion of atmospheric carbon dioxide. The chemical speciation and activity-based supersaturation were determined by the thermodynamic calculation program Visual MINTEQ 3.1 by including all the presented ions in the solution and NaOH that had been used to set up the initial pH. The precipitates were collected at the end of each experiment by vacuum filtration through a 0.2 μm pore size filter (polypropylene membranes). In the case of stopping crystallization reactions, the mixing was stopped and followed by quick filtration to collect the sample. The crystal samples were dried at the room temperature and their weight measured until reaching a stable weight. The water content and dewaterability of samples was measured at room temperature (≈20 °C) based on weight difference of the wet (collected sample after experiment) and dried states. The ion concentrations in the filtrate were determined via spectrophotometry (Hach DR Lange 1900). Solid phases were characterized via powder X-ray diffraction (XRD) (D8 Advance DaVinci, Bruker AXS GmBH) in the range of 2–75° with a step size of 0.013° and a step time of 0.67 s. SEM analyses (Hitachi S-3400N) were performed where samples were placed on carbon tape and sputter coated with gold. The particle size distribution (PSD) was analyzed with a laser diffraction particle size analyzer (Beckman Coulter LS230) in the range of 0.35 to 2,000 μm. The presented particle size distributions are based on dynamic light scattering technique and derived based on sphericity of the particles. Thus, the presented results are the nominal size of crystals for the comparison of the results. The filterability of the products was compared by filtering 50 mL of final sample with 0.2 μm filter paper (polypropylene membrane) under the same vacuum pressure for qualitative comparison.

Preparation of solutions

Stock solutions of $CaCl_2$, $MgCl_2{\cdot}6H_2O$), $NaH_2PO_4{\cdot}2H_2O$ and NH_4Cl were prepared from their corresponding crystalline solids (Merck, reagent grade) using MQ-water. The solution concentrations in this study were selected based on sludge dewatering sidestreams at a municipal wastewater treatment plant. The feed to the digester is a mixture of the thickened primary sludge and dewatered sludge that resulted from the EBPR process. Synthetic concentrate sidestream was then prepared from the stock solutions according to the original composition of total ammonium nitrogen (NH_4-N = 745 mg/L) and total phosphate (PO_4-P = 137 mg/L), where the final composition in each experiment was adjusted to achieve the target compositions. The supersaturated solutions with respect to struvite or calcium phosphates were prepared by the addition of magnesium- or calcium-containing solution to synthetic concentrate sidestream under constant stirring.

Equilibrium modeling

The calcium, magnesium and phosphate ions may form ion complexes that lower the effective concentration of free ions in solution. Therefore, the activity-based supersaturation is calculated for each experiment to identify the supersaturated phases and calculate the effective concentration of ions. The thermodynamic calculations of solution speciation were carried out with Visual MINTEQ 3.1 program (Figure S1) and the activity-based supersaturations are calculated by Equation (1) (Mullin 2001):

$$S_a = \left(\frac{\mathrm{IAP}}{K_{\mathrm{sp}}}\right)^{\frac{1}{\nu}} \quad (1)$$

IAP = ion activity product
K_{sp} = thermodynamic solubility product
ν = number of moles in one mole of solute

The experimental P-recovery yield and the theoretical value are calculated based on Equation (2):

$$\text{P-recovery (\%)} = \left(\frac{\mathrm{P_{initial}} - \mathrm{P_{final}}}{\mathrm{P_{initial}}}\right) \times 100 \quad (2)$$

The supersaturated solid phases based on thermodynamic modeling and under current experimental conditions are identified as $MgNH_4PO_4{\cdot}6H_2O$ (struvite), $Mg_3(PO_4)_2$ (magnesium phosphate) and $MgHPO_4{\cdot}3H_2O$ (magnesium hydrogen phosphate) in the struvite precipitation experiments. In the calcium phosphate experiments the supersaturated phases are amorphous calcium phosphate, $CaHPO_4$ (dicalcium phosphate), $CaHPO_4{\cdot}2H_2O$ (brushite), $Ca_8H_2(PO_4)_6{\cdot}5H_2O$ (octacalcium phosphate, OCP) and $Ca_{10}(PO_4)_6(OH)_2$ (hydroxyapatite, HAP). Table S1 presents the overview of targeted products in this study. The formation of calcium phosphates is reported in the literature as a complex phenomenon by formation of multiple possible phases (Tsuge *et al.* 2002; Ferreira *et al.* 2003; Mekmene *et al.* 2009). Temperature, supersaturation, reaction pH, ionic strength and the presence of impurities affect the out coming phase (Lundager Madsen & Thorvardarson 1984). However, in this study doing the experiments at similar temperature and in the synthetic mode limits the governing parameters to supersaturation and reaction pH.

Design of experiments

The experiments are designed in desupersaturation mode since the different growth kinetics of calcium phosphates and struvite requires distinct experimental conditions for seeded growth experiments (seed amount and mixing). For the calcium phosphate precipitation experiments the Ca:P molar ratios of 1:1 and 1.67:1, and for the struvite experiments Mg:P molar ratios of 1:1 and 1.67:1, are selected. The Ca:P = 1 represents the minimum addition of calcium with respect to phosphate and Ca:P = 1.67:1 is selected to provide the equivalent molar Ca:P for the precipitation of HAP at the startup of the experiment. The Mg:P = 1 is the stoichiometric ratio in struvite and Mg:P = 1.67:1 is selected based on preliminary experiments to optimize the magnesium addition. The calcium phosphate precipitation is investigated in the pH range of 6.5–10.5 and struvite in the pH range of 7.5–9.5 with one pH-unit step. The experiments are designed in two modes: (1) drifting pH: without pH control to extend solid–liquid equilibration to 300 minutes and to compare with equilibrium modeling calculations and (2) constant pH: by keeping the reaction pH constant for 60 minutes. The results of drifting mode experiments are used to assess the thermodynamic equilibrium calculations and to identify the startup of phase transformation by slope changes in pH graphs. All experiments were performed in duplicate.

RESULTS AND DISCUSSION

Phosphorus recovery

The theoretical yield of phosphorus recovery at each experimental condition was calculated using thermodynamic software Visual MINTEQ 3.1. In these calculations, P_{final} is determined by the solubility of struvite and HAP, which is the thermodynamically most stable phase in the corresponding pH range and is constant under constant temperature. $P_{initial}$ is equal in all conditions in terms of total concentration; however, the effective initial concentration that determines the precipitation yield varies highly with solution pH. The equilibrium calculations assume precipitation of pure HAP with the theoretical yield and neglect the reaction kinetics. However, in calcium phosphate precipitation, kinetic factors play equally important roles in determining the precipitating phase (Wang & Nancollas 2008). It is well known that the final product may differ from the thermodynamically most stable one, where kinetically favored phases precipitate earlier according to Ostwald's rule of stages and transform to more stable ones under sufficient driving force (Muster *et al.* 2013). Therefore, a series of experiments in drifting pH mode were performed to compare the experimental P-recovery yield with the theoretical value, and results are presented in Figure 1.

The experimental results show that phosphorus recovery at Ca:P = 1:1 molar ratio does not significantly change by increasing the pH beyond 8.5 (Figure 1(a)). This is because the calcium concentration with respect to phosphorus is the limiting factor and the precipitated phase is the same (i.e. HAP), so further increase of P-recovery requires higher Ca:P molar ratios. It was observed that increase of Ca:P molar ratio to 1.67:1 significantly increased the phosphorus recovery and the increment was more significant for lower pH values. A long induction time (≈ 3 h) was observed for the experiment Ca:P = 1.67:1 at pH = 6.5, which is another reason for difference between the equilibrium and experimental P-recovery. The results show that increasing the Ca:P molar ratio beyond 1.67:1 and pH = 9.5 does not improve the phosphorus recovery in the corresponding experimental conditions (Figure 1(a)). In the case of struvite precipitation, Figure 1(b) shows that the increase of pH improves the P-recovery more than increasing the Mg:P molar ratio. This is because in the range of pH = 7.5–9.5 the HPO_4^- and $H_2PO_4^{2-}$ are the most abundant phosphate species and increase of pH will increase the PO_4^{3-} concentration as the final phosphate species in the struvite crystal along with decrease of struvite solubility. Increasing the Mg:P molar ratio did not significantly improve the P-recovery at pH = 7.5 during 60 minutes of reaction time due to slow precipitation kinetics at low pH. The faster reaction kinetics at higher pH values is the main reason that the experimental values of P-recovery were closer to the theoretical yield.

The role of starting pH on precipitation of different calcium phosphates is significant since pH governs the ion activities and ion complexation that further affect the supersaturation (Zhu *et al.* 2017). The results show that the increase of reaction pH and molar ratios (Ca:P or Mg:P) increases the supersaturation with respect to calcium phosphates and struvite (Figure S1). The increase of supersaturation, as the driving force for precipitation, increases the final P-recovery; however the equivalent

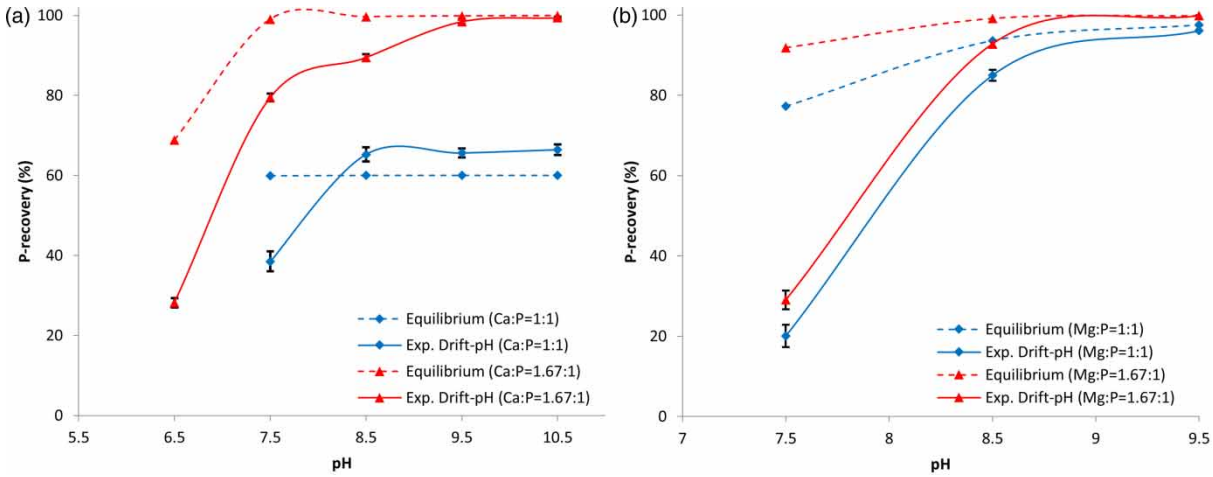

Figure 1 | Percent phosphorus recovery calculated from equilibrium modeling and measured in drifting pH experiments for (a) calcium phosphate (HAP) and (b) struvite precipitation under varying experimental conditions.

P-recovery based on HAP precipitation is only obtained at pH ≥ 9.5. This can result from either slow reaction kinetics or nonstoichiometric precipitation due to low crystallinity of HAP or presence of multiple phases with changing Ca:P ratios in the precipitate. To investigate this, the precipitates were characterized by XRD and SEM analysis at different time points (Figure 2, panel 1). The XRD results show that HAP is the final precipitated product for pH = 7.5–10.5. At pH = 6.5, the initially precipitating phase was characterized as brushite without further phase transformation (Figure 2, panel 1(a)). Figure 2, panel 1(b), shows that at pH = 7.5, a mixture of brushite and HAP was present initially, which then completely transformed to HAP. In the presence of a thermodynamically more stable phase, metastable phases go under transformation and, in solution, this process mostly follows a dissolution–reprecipitation mechanism (Johnsson & Nancollas 1992). The multi-step precipitation behavior at pH = 7.5 can also be observed from the pH change as a function of time during the reaction (Figure S3). The control of the precursor phase and phase transformations is important for wastewater applications since different phases have different potentials for P-recovery and adsorbing impurities. Although OCP is also a supersaturated phase in these experiments, it was not detected by XRD analysis. The precipitated phases for pH ≥8.5 are identified as HAP from the initial time points of the reaction and no phase transformation was observed for these experiments (Figure 2, panel 1(c)).

The results of struvite experiments show that the precipitated phase in all experiments is struvite. The phosphorus recovery increases by increasing the reaction pH. The XRD spectra of precipitated struvite at different pH values corresponds to different morphology of struvite crystals (Figure 2, panel 2). The crystals at pH = 7.5 showed a well-faceted morphology (bipyramidal). Further increase of pH to 8.5 produced hopper crystals (X-shape) and the dendritic crystals observed at pH = 9.5 (Figure 2, panel 2). A detailed insight into the development of different struvite morphologies is given in our recent publication (Shaddel *et al.* 2019).

Constant pH mode

The full-scale crystallization processes are mainly practiced at constant pH. The neutralization of H^+ by

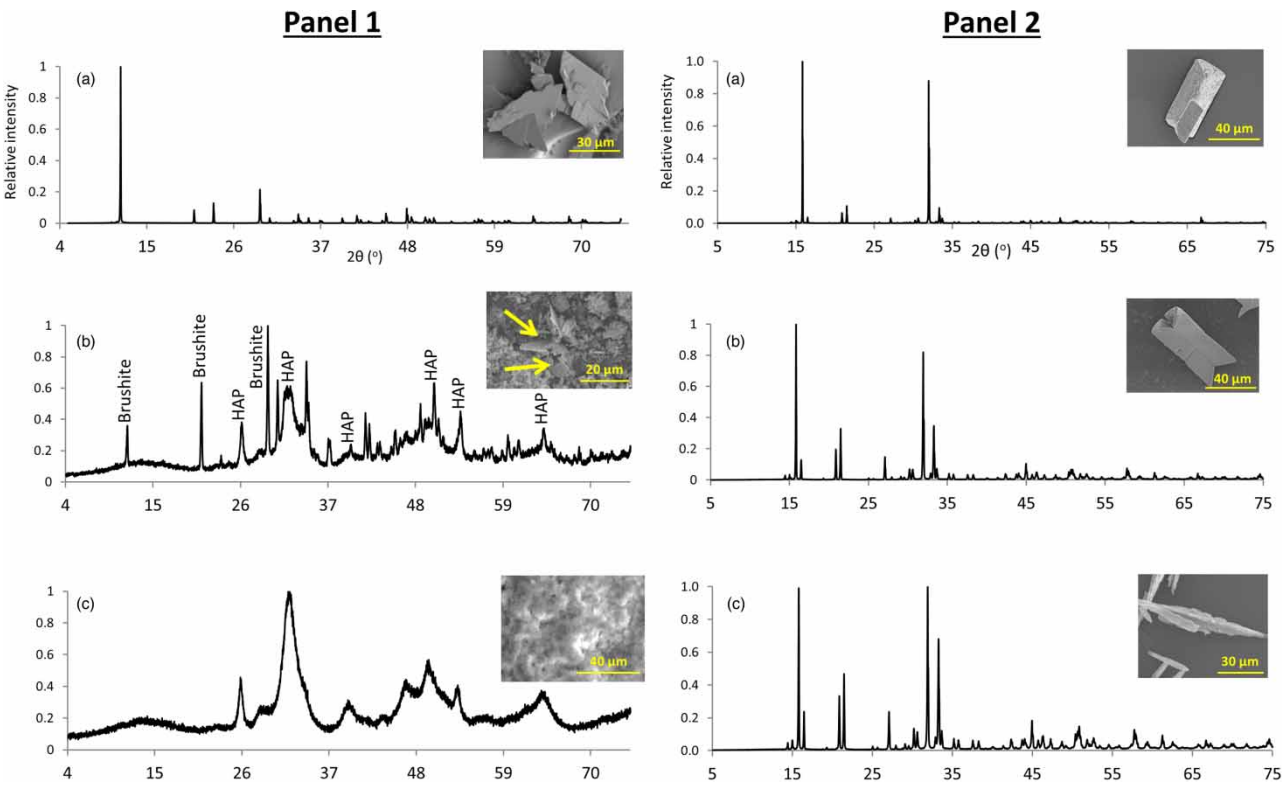

Figure 2 | The XRD spectra and SEM images. Panel 1: (a) Brushite at pH = 6.5 as single-phase, (b) mix of brushite and HAP at pH = 7.5 during the first 20 minutes of precipitation (the arrows point out brushite particles among HAP particles) and (c) HAP at pH ≥ 8.5; Panel 2: (a) pH = 7.5, (b) pH = 8.5 and (c) pH = 9.5 with Mg:P = 1:1 molar ratio.

addition of alkali and keeping a constant pH keeps the driving force for deprotonation of phosphate species. This strategy retains higher precipitation rates to achieve the final recovery in shorter time, so the same series of experiments were designed at constant pH and the results are presented in Figure 3. The phosphorus recovery for both calcium phosphates and struvite increases with increasing the reaction pH. The results show that for the same reaction pH and molar ratio, the final P-recovery is higher with struvite precipitation than with calcium phosphates. In addition to the potential for phosphorus recovery, the product properties are also important in the phosphorus recovery process. Moreover, particle size and purity are important factors that define the value and application of the final product.

The XRD analysis confirmed that for constant pH experiments under the experimental conditions in this study, the final product was HAP when adding $CaCl_2$ and struvite when adding $MgCl_2$ (data not shown). The observed morphology of crystals by SEM showed similar results as presented in Figure 2. In full-scale applications there is a tradeoff between maximum P-recovery and product properties, because pH values higher than 8.5 and low Ca:P molar ratios may trigger the coprecipitation of carbonates and magnesium phosphate (Monballiu *et al.* 2018).

Particle size distribution

In the nutrient recovery by crystallization the uniform distribution of big particles with minimum contribution of fine particles is favorable (Li *et al.* 2019). The bigger particles will settle faster and bring fewer challenges in post-handling like drying and filtration, while fine particles will settle slower, and increase the chance of wash-out from reactor, especially in fluidized bed reactors. Thus, the product properties are important parameters in design and operation of the crystallizer, which require an overall optimization for P-recovery and particle size.

The PSD of obtained crystals is presented in Figure 4. Differences in the PSD and median size of the final products under different reaction conditions can be explained by the different levels of initial supersaturation, different degrees of aggregation and possible phase transformation for calcium phosphate experiments. Supersaturation is the main driving force for the crystallization process and highly influences particle size and size distribution due to its strong effect on the nucleation and growth rates. Smaller particles observed with increasing initial supersaturation result from boosted nucleation rates that produce higher number of particles (Mehta & Batstone 2013). Then, division of the remaining supersaturation for growth of many particles leads to production of particles with smaller size at the end of the experiment. In the case of calcium phosphate crystallization, median size does not decrease significantly with increasing initial supersaturation at higher pH values. This is probably due to aggregation of the produced particles that compensate for the higher nucleation rate at higher supersaturations (Collier & Hounslow 1999; Andreassen & Hounslow 2004). It can be observed that for both the Ca:P molar ratios the median size of the produced particles at $pH = 7.5$ is two times bigger than the produced particles at $pH \geq 8.5$. This is because the initial phase is brushite with further transformation to HAP, and lower nucleation rates,

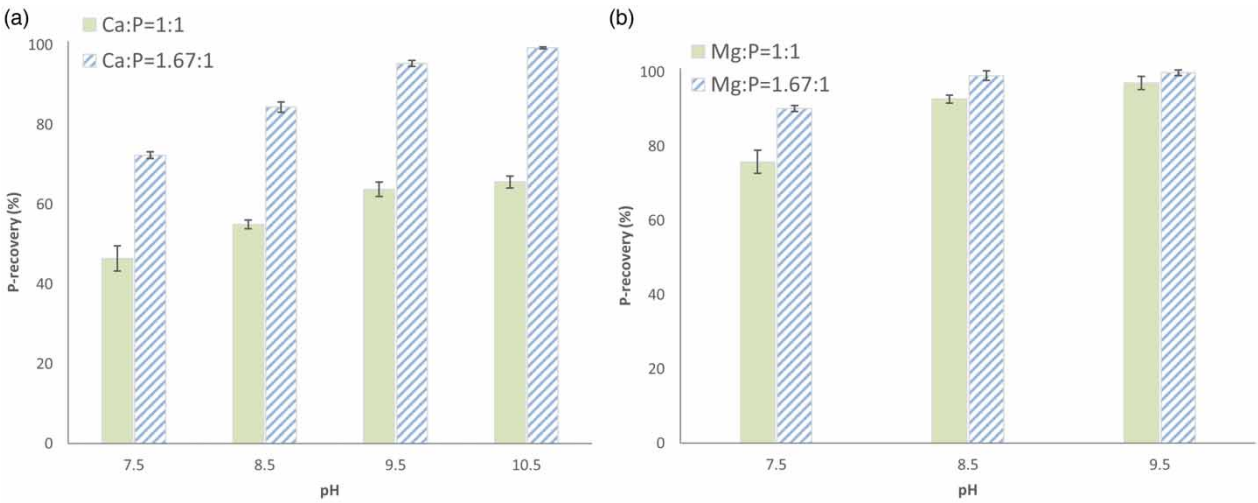

Figure 3 | Experimental values for phosphorus recovery in constant pH experiments with the precipitation of (a) hydroxyapatite and (b) struvite.

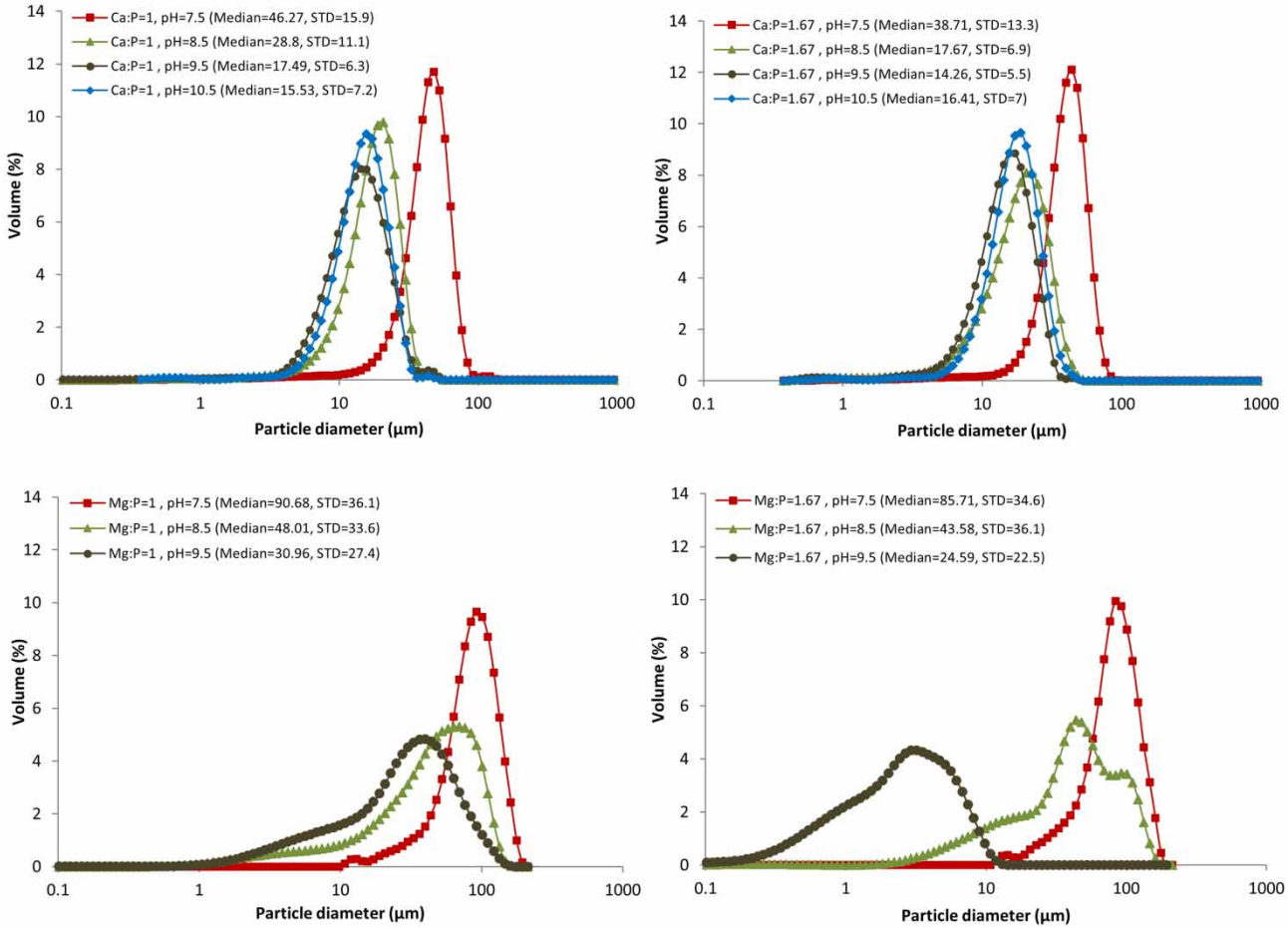

Figure 4 | Particle size distribution and median particle size for calcium phosphate experiments (final product as HAP) and struvite particles at constant pH and different operational conditions (STD: standard deviation).

which can explain the bigger particle size in this case (Ucar *et al.* 2017).

The desired size of crystals mostly depends on their final use. The less brittle crystals are desirable for agricultural purposes as they can be used by current fertilizer spreading machines. The bigger and denser crystals facilitate the handling and shipping. On the other hand when it comes to release rate, the smaller particles have higher release rates due to their high surface area/volume ratio (Forrest *et al.* 2008; Muster *et al.* 2013).

An easily filterable and washable product is desirable in wastewater applications. The filterability depends on PSD but this dependence is complicated (Liu & Qu 2016). In our experiments, the filterability followed the trend of struvite > brushite > HAP. The PSD at pH = 7.5 for different molar ratios resulted in the best filterability, which corresponds to the narrow size distribution and largest median particle. Increasing the reaction pH lowers the homogeneity of PSD and this effect is more pronounced for the struvite particles (Figure 4). Generally, the crystals with narrow PSD and larger size show better filterability of crystalline product (Liu & Qu 2016). The homogeneity of size distribution is more important in determining the filterability. The filling of the voids between the larger particles will reduce the overall porosity and consequently lower the filterability of the product (Dorf 2004). The average standard deviation of PSD for struvite was 35.1 μm at pH = 7.5 and 8.5, and 25 μm at pH = 9.5. The higher standard deviation at lower pH is due to the effect the initial supersaturation has on the aggregation of struvite crystals. The aggregation of struvite crystals is higher at lower initial supersaturation (i.e. pH = 7.5 and pH = 8.5), and no aggregation was observed at high initial supersaturation (i.e. pH = 9.5) (Shaddel *et al.* 2019). The average standard deviation of PSD for calcium phosphates was 14.6 μm at pH = 7.5 and 7.0 μm at pH ≥ 8.5. The lower homogeneity of the obtained

calcium phosphate particles at pH = 7.5 is due to phase transformation of brushite to HAP. Therefore, the solid retention time should be appropriately determined to obtain a more homogeneous product in full-scale reactors.

Water content

The settleability and water content of the product are important factors for agricultural applications (e.g. no humidity, no reactivity) (Egle *et al.* 2016). For wastewater applications, higher water content means lower purity of final product. Figure 5 shows the percent water content for calcium phosphates and struvite precipitated at different pH values. The average water content trend is HAP (48%) > brushite (23%) > struvite (8%).

The average dewaterability rate of struvite at room temperature was better than CaP products and in the order of struvite (1.5 days), brushite (2 days), HAP (4 days). The dewaterability rate, in addition to the type of the product, depends on the particle size. The struvite particles have bigger size than the calcium phosphate particles. The smaller particles have larger surface area, so their water content would be higher and consequently longer time is required for dewatering of the product. The final product of all experiments at pH > 7.5 is HAP. However, the HAP that resulted from transformation of brushite at pH = 7.5 showed lower water content than HAP that directly precipitated at higher pH values. The product at pH = 9.5 consisted of big flocs, which results in highest water content among calcium phosphates (Figure S4).

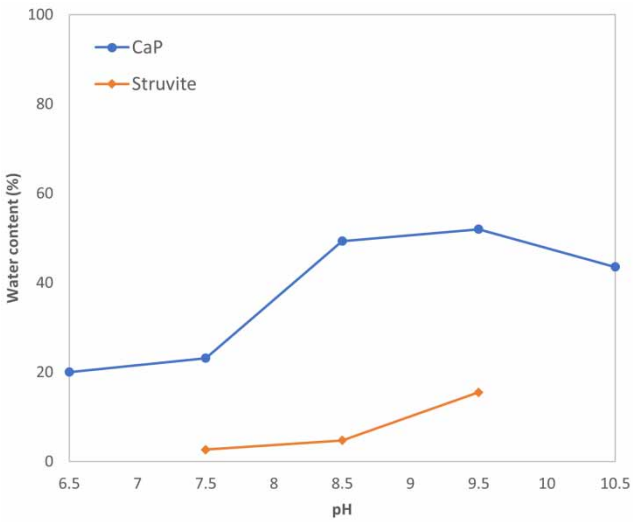

Figure 5 | The percent water content of different products for Ca/Mg:P = 1:1 molar ratio.

Economics and application as fertilizer

The chemical cost constitutes an important fraction of the operational costs. It represents a major part of the overall struvite production cost and is deterministic on payback time (Vaneeckhaute *et al.* 2017; Li *et al.* 2019). Therefore, an economic evaluation was performed by considering the chemical consumption (i.e. $CaCl_2$, $MgCl_2$ and NaOH) based on the experiments in this study. The cost of electricity (8.1% of the total costs) and operational and maintenance costs (16% of the total costs) were acquired from a full-scale struvite reactor. The total cost for each case was calculated by Equation (3) which is related to 1 kg of phosphorus recovered and presented in Figure 6. The total cost in the presented economic evaluation should be considered for comparison purposes, as the total cost in full scale would be lower due to a lower chemical costs in big scale.

$$\text{Total cost} = \text{chemical costs} + \text{electricity costs} + \text{operational and maintenance costs} \quad (3)$$

The chemicals used as Ca^{2+} and Mg^{2+} source and the chemical cost for pH adjustment are major expenses in the P-recovery process by calcium phosphate or struvite precipitation. The results show that the molar ratio of Ca:P or Mg:P = 1.67:1 and pH = 8.5 are the optimum reaction conditions with respect to the cost and P-recovery efficiency for both struvite and calcium phosphates. The combination of $Ca(OH)_2$ and $CaCl_2$ may further reduce the chemical cost since $Ca(OH)_2$ is less expensive than $CaCl_2$ while providing the source for both calcium and pH adjustment. The price of $MgCl_2$ is higher than $CaCl_2$ and the amount of NaOH used for pH control in struvite precipitation was higher than for calcium phosphate. Increasing the pH beyond 8.5 is not cost-effective as high buffer capacity of phosphate ion implies addition of considerably higher amount of NaOH. In this study the base requirement for adjustment of initial pH to 9.5 and 10.5 was respectively 3.3 and 6.2 times higher than base requirement for pH = 8.5.

Calcium phosphates and struvite are potentially secondary resource materials for the phosphorus industry. However, the agronomic effectiveness of recovered product depends on its final use and soil characteristics. Therefore, the economic value and the desired characteristics for struvite or calcium phosphate precipitates should be thoroughly investigated based on process requirements and final application. From the application perspective, the fertilizer value of struvite is higher than the products in the calcium phosphate family since struvite contains N and P as primary

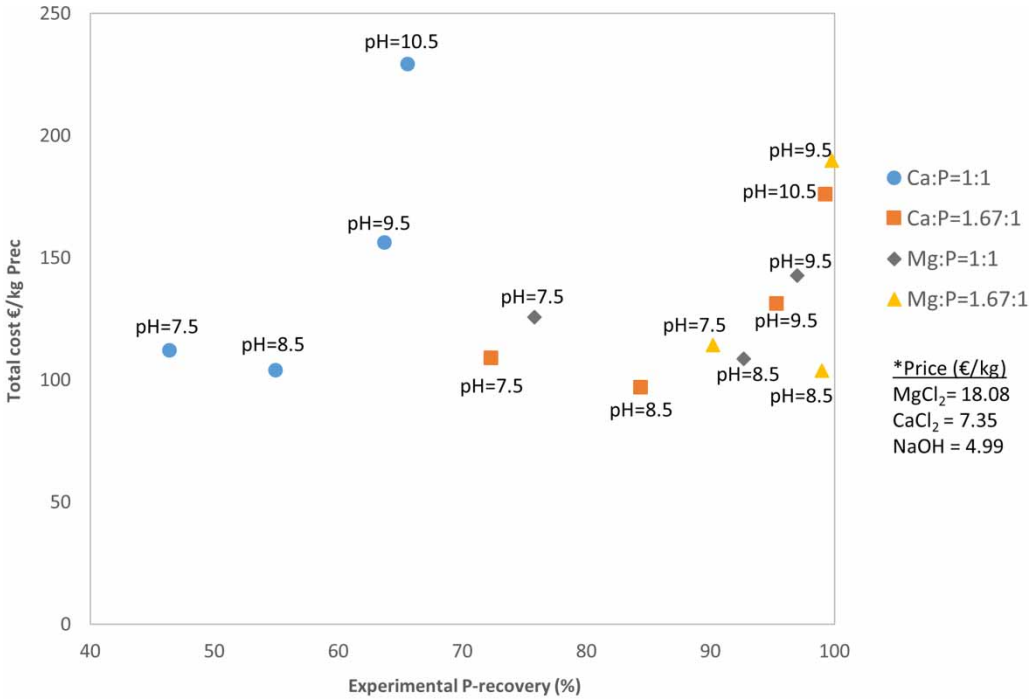

Figure 6 | The calculated total cost for different operational conditions in euros per kg phosphorus recovered (€/kg Prec). *Price quoted by VWR international, for technical grade material in 25 kg bag (September 2018).

macronutrients and Mg as secondary macronutrient. However, the calcium phosphate products are better alternatives as raw materials for production of artificial fertilizers since the magnesium in the struvite may interfere with the chemical processes based on sulfuric acid for production of NPK artificial fertilizer (Van Nieuwenhuyse 2000). In the case of comparison based on fertilizer potential, generally struvite is preferred over HAP. The slow release rate of struvite lowers the chance of rapid leaching and allows the plants to take up the nutrients, so less frequent application is needed (Caddarao *et al.* 2018). The fertilizer efficiency of calcium phosphates and struvite has been investigated by several researchers. There are several studies that reported struvite effectiveness is the same as the effectiveness of monocalcium phosphate for plant growth, and of diammonium phosphate and superphosphate for crop growth (Ghosh *et al.* 1996; Hao *et al.* 2013). Römer & Steingrobe (2018) evaluated 32 recycled P-products and they reported struvite as a good fertilizer with proper availability for plants.

Evaluation of the proposed strategy (case study)

A wastewater treatment plant with EBPR was considered as a case study to evaluate the performance of the proposed alternative strategy. The reject composition that has been used in this study imitates the current reject composition in the plant. However, mass balance calculations and different scenarios for P-recovery were used to evaluate the performance of the proposed strategy under a more generic condition. Figure 7 shows the simplified flow chart for the intended plant. The four feasible scenarios for P-recovery on the sludge dewatering sidestreams were defined as: (1) without P-stripper via mixed reject, (2) without P-stripper on post-digested reject, (3) with P-stripper via post-digested reject and (4) with P-stripper via calcium phosphate on pre-digested reject and via struvite on post-digested reject.

First, it should be noticed that application of P-stripper is necessary since exclusion of the P-stripper in scenario 1 and 2 implies significant reduction of P-recovery potential and operational problems. The operational problems can be uncontrolled struvite precipitation in the anaerobic digester, and clogging in downstream pipes and post-digestion dewatering equipment. In addition, mixing the two reject streams in scenario 1 is not favorable as it reduces the phosphorus concentration in the mixed flow, which reduces the P-recovery potential. However, the pre-digestion sidestream should be considered for P-recovery as it contains considerable amount of the soluble phosphorus, and return of this flow to the inlet of the plant will increase the phosphorus load to the biological treatment stage. The ultimate

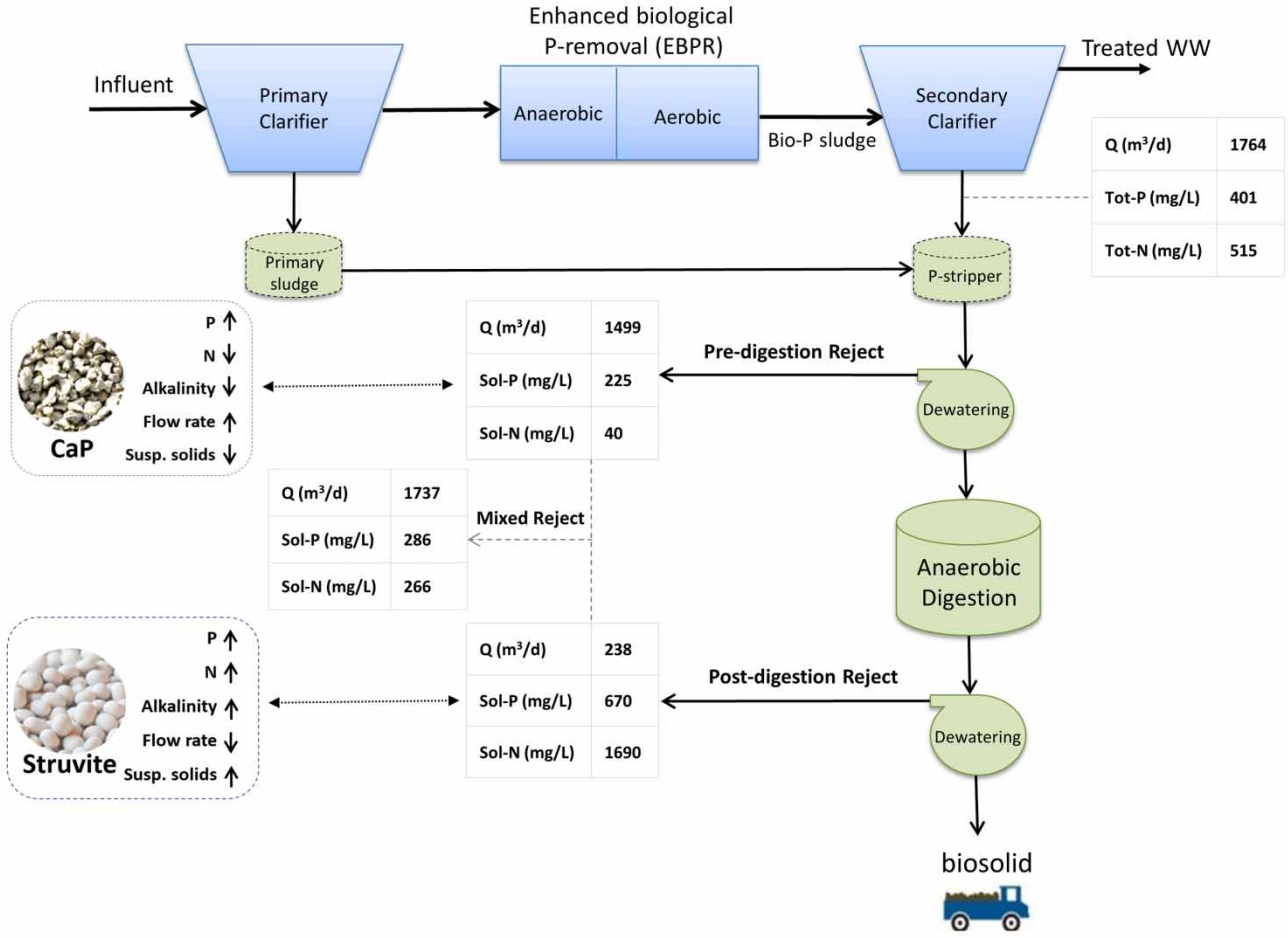

Figure 7 | The simplified flow chart for a wastewater treatment with enhanced biological phosphorus removal and mass balance data for the targeted streams.

comparison of scenario 3 and 4 in this case study requires dedicated experimental data, while the equilibrium P-recovery calculations were used for comparison purposes. It was noticed that the overall P-recovery in scenario 4 depends on the P-recovery efficiency on pre-digestion reject. The associated costs for recovery of 1 kg P in scenario 4 were 40–60% lower than scenario 3, whereas using a mix of $CaCl_2$ and $Ca(OH)_2$ can further reduce the costs in scenario 4. This is because $Ca(OH)_2$ is less expensive than $CaCl_2$ and it can be used to increase Ca:P molar ratio and pH at a lower cost. Assuming that product value would be tied to phosphorus content, brushite is a better option for pre-digestion P-recovery due to higher P-content and lower transport cost.

Therefore, it can be concluded that customizing the product based on sidestream characteristics, in addition to operational benefits, has a great potential to improve efficiency and financial sustainability of the phosphorus recovery process. However, it should be noted that there is not a one-size-fits-all solution and process requirements along with local needs should be considered in identification of an ideal process solution.

CONCLUSION

The results of this study show that introducing diversity in the final products of the phosphorus recovery process is an effective approach to improve the value chain for recovered phosphorus. In addition, it increases the flexibility in handling different types of sludge dewatering sidestreams. It was shown that both struvite and calcium phosphates are proper alternatives for phosphorus recovery from phosphate-rich sidestreams in the EBPR process. However, the final choice among these products mainly depends on process requirements and final application of the recovered product. Supersaturation as an inclusive parameter can be used for optimization of phosphorus recovery by crystallization as it governs both the recovery efficiency and reaction

kinetics. The effective regulation of supersaturation is achievable by adjustment of the reaction pH and chemical dosing of magnesium and calcium. It is concluded that phase transformation should be considered for calcium phosphate crystallization since it affects the purity, particle size and dewaterability of the final product. The overall optimum pH for both struvite and calcium phosphate precipitation, by considering both recovery efficiency and economic feasibility, was found to be pH = 8.5. The low pH values result in slow precipitation rates and high pH values trigger the nucleation and production of fine particles. The struvite has lower water content and better dewaterability than calcium phosphates. However, under the same operational conditions, the chemical expenses for phosphorus recovery by calcium phosphate precipitation are lower than those of struvite.

FUNDING

We gratefully acknowledge financial support provided by Research Council of Norway (RECOVER project) and our partners: Cambi, Kemira, Krüger Kaldnes, Norconsult, Salsnes Filter and Doscon.

NOTES

The authors declare no competing financial interest.

REFERENCES

Andreassen, J. P. & Hounslow, M. J. 2004 Growth and aggregation of vaterite in seeded-batch experiments. *AIChE J.* **50**, 2772–2782. https://doi.org/10.1002/aic.10205.

Caddarao, P. S., Garcia-Segura, S., Ballesteros, F. C., Huang, Y. H. & Lu, M. C. 2018 Phosphorous recovery by means of fluidized bed homogeneous crystallization of calcium phosphate. Influence of operational variables and electrolytes on brushite homogeneous crystallization. *J. Taiwan Inst. Chem. Eng.* **83**, 124–132. https://doi.org/10.1016/j.jtice.2017.12.009.

Chipasa, K. B. 2003 Accumulation and fate of selected heavy metals in a biological wastewater treatment system. *Waste Manage.* **23**, 135–143. https://doi.org/10.1016/S0956-053X(02)00065-X.

Cichy, B., Kużdżał, E. & Krztoń, H. 2019 Phosphorus recovery from acidic wastewater by hydroxyapatite precipitation. *J. Environ. Manage.* **232**, 421–427. https://doi.org/10.1016/j.jenvman.2018.11.072.

Collier, A. P. & Hounslow, M. J. 1999 Growth and aggregation rates for calcite and calcium oxalate monohydrate. *AIChE J.* **45**, 2298–2305. https://doi.org/10.1002/aic.690451105.

Cornel, P. & Schaum, C. 2009 Phosphorus recovery from wastewater: needs, technologies and costs. *Water Sci. Technol.* **59**, 1069–1076. https://doi.org/10.2166/wst.2009.045.

Dorf, R. C. 2004 *The Engineering Handbook*, 2nd edn. CRC Press, New York, USA.

Egle, L., Rechberger, H., Krampe, J. & Zessner, M. 2016 Phosphorus recovery from municipal wastewater: an integrated comparative technological, environmental and economic assessment of P recovery technologies. *Sci. Total Environ.* **571**, 522–542. https://doi.org/10.1016/j.scitotenv.2016.07.019.

Ferreira, A., Oliveira, C. & Rocha, F. 2003 The different phases in the precipitation of dicalcium phosphate dihydrate. *J. Cryst. Growth* **252**, 599–611. https://doi.org/10.1016/S0022-0248(03)00899-6.

Forrest, A. L., Fattah, K. P., Mavinic, D. S. & Koch, F. A. 2008 Optimizing struvite production for phosphate recovery in WWTP. *J. Environ. Eng.* **134**, 395–402. https://doi.org/10.1061/(ASCE)0733-9372(2008)134:5(395).

Frossard, E., Bauer, J. P. & Lothe, F. 1997 Evidence of vivianite in $FeSO_4$-flocculated sludges. *Water Res.* **31**, 2449–2454. https://doi.org/10.1016/S0043-1354(97)00101-2.

Gerardi, M. H. 2003 *The Microbiology of Anaerobic Digesters*. https://doi.org/10.1016/S0140-6736(05)61039-2.

Ghosh, G. K., Mohan, K. S. & Sarkar, A. K. 1996 Characterization of soil-fertilizer P reaction products and their evaluation as sources of P for gram (*Cicer arietinum* L.). *Nutr. Cycl. Agroecosyst.* **46**, 71–79. https://doi.org/10.1007/BF00210225.

Gould, M. S., G. F. J. 1977 Heavy metal distribution in anaerobically digested sludges. In *30th Industrial Waste Conference*.

Hao, X., Wang, C., Van Loosdrecht, M. C. M. & Hu, Y. 2013 Looking beyond struvite for P-recovery. *Environ. Sci. Technol.* **47**, 4965–4966. https://doi.org/10.1021/es401140s.

Johnsson, M. S. A. & Nancollas, G. H. 1992 The role of brushite and octacalcium phosphate in apatite formation. *Crit. Rev. Oral Biol. Med.* https://doi.org/10.1177/10454411920030010601.

Law, K. P. & Pagilla, K. R. 2018 Phosphorus recovery by methods beyond struvite precipitation. *Water Environ. Res.* **90**, 840–850. https://doi.org/10.2175/106143017X15131012188006.

Li, Z., Tabanpour, M. & Forstner, G. 2018 Comparison of phosphorus recovery through pre-anaerobic-digestion brushite precipitation and post-anaerobic-digestion struvite crystallization. In *WEF Nutrient Removal and Recovery Conference*.

Li, B., Boiarkina, I., Yu, W., Huang, H. M., Munir, T., Wang, G. Q. & Young, B. R. 2019 Phosphorous recovery through struvite crystallization: challenges for future design. *Sci. Total Environ.* **648**, 1244–1256. https://doi.org/10.1016/j.scitotenv.2018.07.166.

Liu, Y. & Qu, H. 2016 Design and optimization of a reactive crystallization process for high purity phosphorus recovery from sewage sludge ash. *J. Environ. Chem. Eng.* **4**, 2155–2162. https://doi.org/10.1016/j.jece.2016.03.042.

Lundager Madsen, H. E. & Thorvardarson, G. 1984 Precipitation of calcium phosphate from moderately acid solution. *J. Cryst. Growth* **66**, 369–376. https://doi.org/10.1016/0022-0248(84)90220-3.

Marcato, C. E., Pinelli, E., Pouech, P., Winterton, P. & Guiresse, M. 2008 Particle size and metal distributions in anaerobically digested pig slurry. *Bioresour. Technol.* **99**, 2340–2348. https://doi.org/10.1016/j.biortech.2007.05.013.

Massé, D. I., Croteau, F. & Masse, L. 2007 The fate of crop nutrients during digestion of swine manure in psychrophilic anaerobic sequencing batch reactors. *Bioresour. Technol.* **98**, 2819–2823. https://doi.org/10.1016/j.biortech.2006.07.040.

Mehta, C. M. & Batstone, D. J. 2013 Nucleation and growth kinetics of struvite crystallization. *Water Res.* **47**, 2890–2900. https://doi.org/10.1016/j.watres.2013.03.007.

Mehta, C. M., Khunjar, W. O., Nguyen, V., Tait, S. & Batstone, D. J. 2015 Technologies to recover nutrients from waste streams: a critical review. *Crit. Rev. Environ. Sci. Technol.* **45**, 385–427. https://doi.org/10.1080/10643389.2013.866621.

Mekmene, O., Quillard, S., Rouillon, T., Bouler, J.-M., Piot, M. & Gaucheron, F. 2009 Effects of pH and Ca/P molar ratio on the quantity and crystalline structure of calcium phosphates obtained from aqueous solutions. *Dairy Sci. Technol.* **89**, 301–316. https://doi.org/10.1051/dst/2009019.

Melia, P. M., Cundy, A. B., Sohi, S. P., Hooda, P. S. & Busquets, R. 2017 Trends in the recovery of phosphorus in bioavailable forms from wastewater. *Chemosphere* **186**, 381–395. https://doi.org/10.1016/j.chemosphere.2017.07.089.

Möller, K. & Müller, T. 2012 Effects of anaerobic digestion on digestate nutrient availability and crop growth: a review. *Eng. Life Sci.* **12**, 242–257. https://doi.org/10.1002/elsc.201100085.

Monballiu, A., Desmidt, E., Ghyselbrecht, K. & Meesschaert, B. 2018 Phosphate recovery as hydroxyapatite from nitrified UASB effluent at neutral pH in a CSTR. *J. Environ. Chem. Eng.* **6**, 4413–4422. https://doi.org/10.1016/J.JECE.2018.06.052.

Mullin, J. W. 2001 *Crystallization*. Butterworth-Heinemann, London, UK.

Munir, M. T. T., Li, B., Boiarkina, I., Baroutian, S., Yu, W. & Young, B. R. 2017 Phosphate recovery from hydrothermally treated sewage sludge using struvite precipitation. *Bioresour. Technol.* **239**, 171–179. https://doi.org/10.1016/j.biortech.2017.04.129.

Muster, T. H., Douglas, G. B., Sherman, N., Seeber, A., Wright, N. & Güzükara, Y. 2013 Towards effective phosphorus recycling from wastewater: quantity and quality. *Chemosphere* **91**, 676–684. https://doi.org/10.1016/j.chemosphere.2013.01.057.

Römer, W. & Steingrobe, B. 2018 Fertilizer effect of phosphorus recycling products. *Sustainability* **10**, 1166. https://doi.org/10.3390/su10041166.

Shaddel, S., Ucar, S., Andreassen, J.-P. & Østerhus, S. W. 2019 Engineering of struvite crystals by regulating supersaturation – correlation with phosphorus recovery, crystal morphology and process efficiency. *J. Environ. Chem. Eng.* **7**, 102918.

Thannimalay, L., Yusoff, S. & Zawawi, N. Z. 2013 Life cycle assessment of sodium hydroxide. *Aust. J. Basic Appl. Sci.* **7**, 421–431.

Tsuge, H., Tanaka, Y., Yoshizawa, S. & Kuraishi, T. 2002 Reactive crystallization behaviour of calcium phosphate with and without whey protein addition. *Chem. Eng. Res. Des.* **80**, 105–110. https://doi.org/10.1205/026387602753393277.

Ucar, S., Bjørnøy, S. H., Bassett, D. C., Strand, B. L., Sikorski, P. & Andreassen, J. P. 2017 Transformation of brushite to hydroxyapatite and effects of alginate additives. *J. Cryst. Growth* **468**, 774–780. https://doi.org/10.1016/j.jcrysgro.2016.11.019.

Vaneeckhaute, C., Lebuf, V., Michels, E., Belia, E., Vanrolleghem, P. A., Tack, F. M. G. & Meers, E. 2017 Nutrient recovery from digestate: systematic technology review and product classification. *Waste and Biomass Valorization* **8**, 21–40. https://doi.org/10.1007/s12649-016-9642-x.

Van Nieuwenhuyse, A. E. 2000 *Production of NPK Fertilizers by the Mixed Acid Route*. European Fertilizer Manufacturers' Association, Brussels, Belgium.

Vasenko, L. & Qu, H. 2017 Effect of NH_4-N/P and Ca/P molar ratios on the reactive crystallization of calcium phosphates for phosphorus recovery from wastewater. *J. Cryst. Growth* **459**, 61–66. https://doi.org/10.1016/j.jcrysgro.2016.11.076.

Wan, G., Hu, X., Liu, Y., Han, C., Sood, A. K., Calin, G. A., Zhang, X. & Lu, X. 2013 A novel non-coding RNA lncRNA-JADE connects DNA damage signalling to histone H4 acetylation. *EMBO J.* **32**, 2833–2847. https://doi.org/10.1016/j.scitotenv.2015.08.048.

Wang, L. & Nancollas, G. H. 2008 Calcium orthophosphates: crystallization and dissolution. *Chem. Rev.* **108**, 4628–4669. https://doi.org/10.1021/cr0782574.

Warren, R. G. 1981 Tectonic setting of the easternmost Arunta Block (Australia). *Aust. Bur. Miner. Resour. Geol. Geophys. Rep.* **221**, 1871–1876. https://doi.org/10.13031/2013.33060.

Wilfert, P., Dugulan, A. I., Goubitz, K., Korving, L., Witkamp, G. J. & Van Loosdrecht, M. C. M. 2018 Vivianite as the main phosphate mineral in digested sewage sludge and its role for phosphate recovery. *Water Res.* **144**, 312–321. https://doi.org/10.1016/j.watres.2018.07.020.

Zhu, H., Guo, D. & Qi, W. 2017 Development of Sr-incorporated biphasic calcium phosphate bone cement. *Mater. Res. Express* **4**, 125015. https://doi.org/10.1088/2053-1591/aa9bd3.

First received 17 December 2018; accepted in revised form 13 May 2019. Available online 24 May 2019